

Cooperation dynamics in the networked geometric Brownian motion

Viktor Stojkoski^{1,*}, Zoran Utkovski², Lasko Basnarkov^{1,3}, and Ljupco Kocarev^{1,3†}
¹*Macedonian Academy of Sciences and Arts, P.O. Box 428, 1000 Skopje, Republic of Macedonia*
²*Fraunhofer Heinrich Hertz Institute, Einsteinufer 37, 10587, Berlin, Germany and*
³*Faculty of Computer Science and Engineering,
 Ss. Cyril and Methodius University,
 P.O. Box 393, 1000 Skopje, Republic of Macedonia*

(Dated: December 20, 2024)

Networked geometric Brownian motion with pooling and sharing of resources is developed as a model for the evolution of cooperation in fluctuating environments. The model reveals that, while in general cooperation reduces fluctuations and increases the individual long-run growth rates (i.e. is evolutionary advantageous), the interplay with the network structure may yield large discrepancies in the observed individual resource endowments. We comment on the possible biological and social implications and discuss relations to econophysics.

PACS numbers: 87.23.Ge, 87.23.Kg, 02.50.Ey, 02.50.Le

Introduction – Cooperation has played a fundamental role in the evolution of many levels of networked organizations, ranging from simple cell to complex human interactions [1]. However, natural selection imposes competition and thus cooperative behavior is predicated on the co-occurrence of a specific mechanism within the studied network [2]. A ubiquitous, yet largely unexplored, feature in the cooperative dynamics on complex networks is the presence of a fluctuating environment, i.e. situations where the temporal evolution is strongly affected by relative movement. In such situations, fluctuations have a net-negative effect on the time-averages, although having no effect on the ensemble properties [3]. This observation, which captures the non-ergodicity of fluctuating environments, yields evolutionary behavior which essentially differs from the one observed in standard models [4, 5].

Noisy resource growth is a common model for fluctuations [5–7]. A simple way to account for such environment is to assume that the dynamics of resources of an individual follow a geometric Brownian motion (GBM). An additional advantage of modeling through GBM lies in its universality, as the process represents an attractor of more complex models that exhibit multiplicative growth [8, 9]. Its non-ergodicity is manifested in the difference between the time-average growth rate observed in an individual trajectory, $\mu - \sigma^2/2$, and the ensemble average growth, μ , where μ is the drift and σ is the amplitude of the noise [3, 10]. As the time-average growth rate determines the evolutionary performance of an individual GBM trajectory, it is easily related to real-life phenomena. For instance, in evolutionary game theory the time-average growth rate is the geometric mean fitness for the accumulated payoff (i.e. resources) of a particular phenotype [11]. In economic decision theory, where

wealth (resource) dynamics follows a multiplicative process, the same growth observable arises naturally as the unique utility measure [10].

From an evolutionary perspective, individuals with lower noise amplitude should exhibit higher long-run growth rates and should thus be favored. In this regard, pooling and sharing may constitute a fundamental mechanism for the evolution of cooperation in well-mixed fluctuating environments as it reduces the uncertainties in future growth and, hence, brings closer the observed growth rate to the ensemble value [12–14]. For GBM dynamics, this has been nicely evidenced in [14]. Concretely, the pooling and sharing mechanism can be described as follows. A mutation wires cooperation in a population of N individuals whose resource dynamics follow a GBM trajectory. In this case, the time-average growth rate equals $\mu - \sigma^2/(2N)$. Notice that as the number of cooperating individuals increases, the time-average growth rate converges to the ensemble average growth. This implies that in finite populations, the inclusion of new individuals always produces a net performance gain. As a result, the pooling and sharing mechanism has been linked with the evolution of cooperation at the lowest possible biological level – the transition towards multicellularity, where a species of non-cooperating single cells mutates to a species of multicellular organisms, sharing nutrients through common membranes [15, 16]. Similar analogy may hold at higher levels of intelligence. As an illustration, consider situations where individuals join a community-supported agriculture to exchange their produced goods for a fixed basket of products, thereby reducing the risks in farming [17]. Another example are nations joining unions to assure sustainable economic growth through common goals [18].

Here, we investigate the impact of *complex networks* on the cooperative dynamics in fluctuating environments, by studying the networked GBM with pooling and sharing of resources. While there remains the general trend that cooperation reduces fluctuations (i.e. is evolutionary ad-

* vstojkoski@manu.edu.mk

† lkocarev@manu.edu.mk

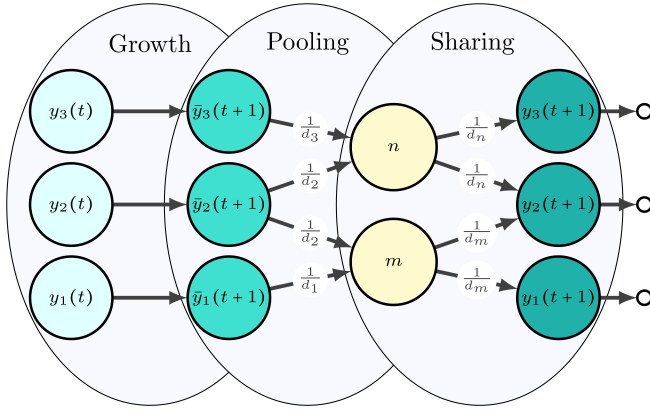


FIG. 1. Networked GBM with pooling and sharing of resources. The resources of three individuals grow according to GBM and after that they are pooled in n and m . Finally, the pools distribute the pooled resources equally among its participants. For visualization purposes we set $dt = 1$.

vantageous), we show that the unique interplay between the non-ergodic fluctuation-generating process and the network topology may generate large discrepancies in the individual resource endowments. When present, this inequality has a negative effect on the growth rates of the individuals, hampering their evolutionary performance. Parallels can be made to current societal discussions on inequality [19].

Model of networked geometric Brownian motion with pooling and sharing of resources – Real-life interactions between individuals are, however, seldom realized in a well-mixed structure, and are instead driven by a complex network of contacts [20]. To model this situation, we characterize each individual i with participation in d_i pools. In a discretized version of the model, each round t begins with a *growth phase* where the resources $y_i(t)$ of i grow to $\bar{y}_i(t + dt)$. The growth phase is followed by a *cooperation phase* where each individual pools an equal fraction of its resources in each of the pools it belongs to. Afterwards, each pool returns an equal fraction of the pooled resources to each individual. The resulting mechanism is illustrated in Fig. 1.

The interaction structure is modeled by a connected bipartite random graph \mathbf{B} between finite sets \mathcal{N} of N individuals and \mathcal{M} of M pools, with binary edge variables $B_{im} \in \{0, 1\}$ between pairs of individuals $i \in \mathcal{N}$ and pools $m \in \mathcal{M}$ ($B_{im} = 1$, indicating participation of i in pool m). The bipartite representation offers a principled way of capturing wider information regarding the group composition and network interactions [21]. In this regard, the model can be related to games of public goods played on networks [21–23].

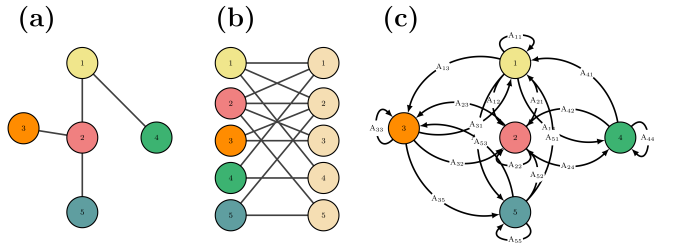


FIG. 2. Graph representation. (a) Example of a random graph with 5 individuals. (b) The bipartite representation modeling interactions in a pooling-sharing game, as used in the numerical experiments. (c) The replacement graph capturing effective reallocation of resources between the individuals. The edges are the non-zero elements of the transition matrix \mathbf{A} , as in equation (2).

By setting $dt \rightarrow 0$, the dynamics can be explained as

$$dy_i = \left[\sum_j^N A_{ij} y_j - y_i \right] dt + \sum_j^N A_{ij} y_j (\mu dt + \sigma dW_j), \quad (1)$$

where dW_j is an independent Wiener increment and \mathbf{A} represents a transition matrix of the network with entries $A_{ij} = \sum_m^M \frac{B_{im}}{d_m} \frac{B_{jm}}{d_j}$ determining the total allocated resources from individual j to individual i . Equation (1) resembles the Bouchaud–Mezard wealth reallocation model [24–27], with the main difference that now the reallocation happens *after* the growth phase.

We formulate the interactions by considering each individual to also be a pool through which its (direct) neighbors share resources. In terms of our formulation, this results in a bipartite graph where the average degree $\langle d \rangle_{\mathcal{N}}$ between individuals is equal to the average degree between pools $\langle d \rangle_{\mathcal{M}}$, i.e. $\langle d \rangle_{\mathcal{N}} = \langle d \rangle_{\mathcal{M}} = \langle d \rangle$. Fig. 2 depicts the process of mapping the original undirected random graph to a directed *replacement* graph, via a bipartite graph representation which models the pooling and sharing mechanism. The edges in the replacement graph capture the elements A_{ij} in the transition matrix \mathbf{A} .

Analytical results – For tractability, we proceed by examining a discrete version of equation (1),

$$y_i(t + \Delta t) = \sum_j A_{ij} y_j(t) \left[1 + \mu \Delta t + \sigma \varepsilon_j(t) \sqrt{\Delta t} \right], \quad (2)$$

where $\varepsilon_j(t)$ is a random variable following the standard Gaussian distribution, and utilize a mean-field approach. For this purpose, we define two variables. First, the grown resources of each individual i are given as

$$\bar{y}_i(t + \Delta t) = y_i(t) \left[1 + \mu \Delta t + \sigma \varepsilon_i(t) \sqrt{\Delta t} \right],$$

For large t the time-average growth rate of this variable should be the same as $g_i(y_i(t), t)$ as its value will be dominated by $y_i(t)$. Second, we define the mean-field around

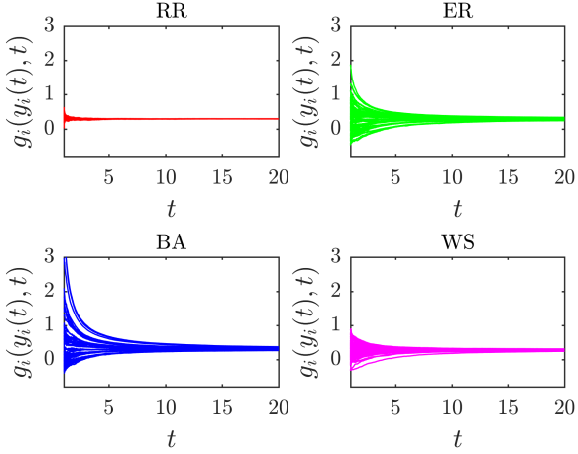


FIG. 3. **Transient regime dynamics.** Individual growth rate dynamics for sample RR, ER, BA and WS graphs. The GBM parameters are set to $\mu = 0.3$ and $\sigma^2 = 0.4$. The results are averaged across 100 realizations of pooling and sharing processes with each graph each having 100 vertices (100 individuals and pools) with an average degree $\langle d \rangle = 5$.

individual i as the average grown resources of each of its neighbors weighted by their contributions to i , i.e.,

$$\langle \bar{y}_i \rangle = \frac{\sum_j A_{ij} \bar{y}_j}{\sum_j A_{ij}}.$$

By combining the last two equations and adapting the time scale such that $\Delta t = 1$, the growth $g_i(y_i(t), t)$ of i can be approximated as

$$g_i(y_i(t), t) = \frac{\log(\sum_j A_{ij})}{t} + \frac{\log(\langle \bar{y}_i \rangle)}{t}. \quad (3)$$

Two implications arise from equation (3). First, in the transient regime there is an additive term in the growth rate which is solely dependent on the network structure. Hence, during this regime, individuals which are better connected in terms of $\sum_j A_{ij}$ should have faster growth rates. The second observation is that the second term on the right-hand side (RHS) of equation (3) eventually converges to the same value for each individual. This is because we study a *connected* graph where participation in a pool implies that there is a path between any pair of individuals. Due to this interconnectedness, we expect that the long run time-average growth of each $\langle \bar{y}_i \rangle$ will be dominated by the growth of the wealthiest individual in the network.

The convergence of the long run growth rates between individuals provides a direct equivalence with the time-average growth rate $g(\langle y \rangle_{\mathcal{N}}, t) = \frac{d \log(\langle y \rangle_{\mathcal{N}})}{dt}$, which is derived from the partial ensemble average $\langle y \rangle_{\mathcal{N}}$. This object is constructed from all individuals present in the network. As a consequence, one can use Itô's lemma to directly calculate the time-average growth rate in the

network. Formally, the lemma states that the differential of an arbitrary one-dimensional function $f(\mathbf{y}, t)$ governed by an Itô drift-diffusion process (such as equation (1)), is given by

$$df(\mathbf{y}, t) = \frac{\partial f}{\partial t} dt + \sum_i \frac{\partial f}{\partial y_i} dy_i + \frac{1}{2} \sum_i \sum_j \frac{\partial^2 f}{\partial y_i \partial y_j} dy_i dy_j. \quad (4)$$

In the case of $g(\langle y \rangle_{\mathcal{N}}, t)$, we have that $f(t, \mathbf{y}) = \log(\langle y \rangle_{\mathcal{N}})$. Then, the first and second derivative of f with respect to y_i and y_j are easily calculated as $\frac{\partial f}{\partial y_i} = \frac{1}{N} \frac{1}{\langle y \rangle_{\mathcal{N}}}$ and $\frac{\partial^2 f}{\partial y_i \partial y_j} = -\frac{1}{N^2} \frac{1}{\langle y \rangle_{\mathcal{N}}^2}$, [28]. Moreover, this transformation makes the differential $df(\mathbf{y}, t)$ ergodic, and since we are looking at long-run averages, dy_i and $dy_i dy_j$ can be substituted with their expected values $\langle dy_i \rangle$ and $\langle dy_i dy_j \rangle$. To estimate these expectations we utilize the independent Wiener increment property $\langle dW_i^2 \rangle = dt$, and make use of the fact that $\sum_k A_{kj} = 1$. Further, we omit terms of order dt^2 as they are negligible. As a result, we obtain that $\langle dy_i \rangle = \left[(1 + \mu) \sum_j A_{ij} y_j - y_i \right] dt$ and $\langle dy_i dy_j \rangle = \sigma^2 dt \sum_k A_{ik} A_{jk} y_k^2$. By inserting the estimates in equation (4) we can approximate the time-average growth rate as

$$g(\langle y \rangle_{\mathcal{N}}, t) = \mu - \frac{\sigma^2}{2} \frac{\langle \hat{y}^2 \rangle_{\mathcal{N}}}{N}, \quad (5)$$

where $\hat{y}_i = y_i / \langle y \rangle_{\mathcal{N}}$ are the rescaled resources of individual i . This is a dimensionless quantity which compares the endowment of resources of an individual with the population average and as such has been particularly useful in analyses related to wealth inequality [24]. In fact, equation (5) indicates that the variance of the rescaled resources $\langle \hat{y}^2 \rangle_{\mathcal{N}}$ dictates the time-average growth rate. Under this model, networks with larger resource inequality, i.e. higher $\langle \hat{y}^2 \rangle_{\mathcal{N}}$, are expected to have lower long-run growth rates than those where the resources are distributed more equally.

When deriving the individual growth rate we utilized an equilibrium property of the system. Such properties are key to understanding the role of complex networks within the pooling and sharing mechanism. In particular, notice that in the limit we can substitute the product of $y_j(t)$ and the exponential of (5) for each $\bar{y}_j(t + \Delta t)$, divide both sides of the equation by the population average resources and conclude that the equilibrium rescaled resources of individual i are

$$\lim_{t \rightarrow \infty} \hat{y}_i(t) = v_i. \quad (6)$$

where v_i is the i -th element of the left-eigenvector of \mathbf{A} associated with the largest eigenvalue normalized in a way such that $\sum_i v_i = N$. A direct corollary is the equilibrium individual growth rate

$$\lim_{t \rightarrow \infty} g_i(y_i(t), t) = \mu - \frac{\sigma^2}{2} \frac{\langle v^2 \rangle}{N}. \quad (7)$$

We emphasize that the quantity on the RHS of equation (7) is always greater than $\mu - \sigma^2/2$. This can be concluded by examining the optimization problem of maximizing $\langle v^2 \rangle$ constrained on $\sum_i v_i = N$, and noting that the global maximum is always less than N . Therefore a network of pooling and sharing individuals on the long run will always outperform non-cooperating GBM trajectories. While this indicates that cooperation is a dominant trait in the population, it also asserts that, depending on the distribution of v , pooling and sharing may produce societies where the distribution of resources differs to a great extent from the one observed in individual trajectories [29].

Numerical results – We numerically evaluate the model properties on four types of random graphs: random d-regular graph (RR) [30], Erdos-Renyi Poisson graph (ER) [31], Watts-Strogatz small-world network (WS) [32] and Barabasi-Albert scale-free network (BA) [33]. Examples for the transient behavior and the convergence properties are given in Fig. 3. To evaluate the differences between well-mixed and networked fluctuating environments we conduct two experiments. In the first experiment, we compare the distribution of the rescaled resources in equilibrium, $P_{\hat{y}}(\hat{y})$, among the graphs. Samples of the corresponding probability density functions (PDFs) are depicted in Fig. 4a. We notice the agreement between the analytical solution in (6) (the value of v_i) and the simulated rescaled resources, \hat{y}_i . We observe that the RR graph exhibits no inequality across the resources (point mass PDF), whereas the PDFs of ER and WS graphs have exponential tails. Finally, the rescaled resources distribution in the BA graph resembles a fat tail. As a consequence, the BA graph has the lowest long run growth rate, followed by ER and WS, as depicted in the inset plot in Fig. 4a.

The second experiment investigates the role of network sparsity (measured through the average degree $\langle d \rangle$), on the wealth distribution. Fig. 4b depicts the variance of rescaled wealth $\langle \hat{y}^2 \rangle$ as function of $\langle d \rangle$. The inset plot gives the ratio of the individual growth rate and the drift parameter, as function of the same variable. We observe that denser ER, WS and BA graphs yield more equal resource distribution compared to their respectively sparser counterparts, whereas in the RR graph the time-average growth is invariant to the average degree.

Our findings suggest that interactions on complex networks play a critical role in the observed time-average growth rates and resource distribution, both in transient regime and in equilibrium. The cooperation dynamics is dictated by the properties of the underlying bipartite

graph which models the network interactions in the pooling and sharing mechanism.

A startling example is the dynamics taking place on a BA scale-free graph, where largest discrepancies between the individual growth-rates are observed in the transient regime, as compared to ER, WS and RR graphs. Furthermore, the BA graph has the smallest time-average growth once the equilibrium is reached, and the most unequal resource distribution. From an evolutionary perspective, a network structure which presents with lower time-average growth may be interpreted as being less supportive to cooperation. It is intriguing whether there is any relationship between the apparent lower propensity to cooperation of BA scale-free networks (under the here considered interaction model) and the recent empirical evidence regarding the low-prevalence (i.e. rarity) of scale-free networks in nature [34, 35].

Conclusions – As a takeaway, we conclude that inequality may arise as a result of the interwoven relationship between complex networks and cooperative dynamics in fluctuating environments. While it is known that certain network topologies promote inequality [33, 36], the effect of cooperative behavior in structured populations is still to be determined [37–39]. As such, our investigations aim at providing deeper understanding on the nature of the relationship between these two occurrences.

Besides providing a basic model of self-reproducing living entities with temporal fluctuations, multiplicative processes are also excessively used to model self-financing investments [40], gambles [10] and wealth allocation [24, 26]. In this respect, our findings may provide insights to economic utility theory with applications to finance, portfolio management, risk-evaluation and decision-making. In addition, they contribute to the ongoing discussions in economics and econophysics regarding the potential negative effects of wealth inequality on economic growth and development [24, 41] and on the individual well-being in general.

A straightforward direction for future work is a scenario where individuals exhibit heterogeneous drifts and volatilities. There, cooperation is evolutionary advantageous only in certain parameter regimes, and thus one should investigate the dynamics under a more general model where individuals are allowed to contribute only a fraction of their resources to the pool. In this context, relations to simplistic behavioral rules that model partial cooperation, e.g. [42, 43], may be of particular relevance.

This research was supported in part by DFG through grant “Random search processes, Lévy flights, and random walks on complex networks”.

[1] R. M. Axelrod, *The evolution of cooperation* (Basic books, 2006).
[2] M. A. Nowak, *Science* **314**, 1560 (2006).
[3] O. Peters and W. Klein, *Physical review letters* **110**, 100603 (2013).
[4] F. Radicchi and C. Castellano, *Physical Review Letters* **120**, 198301 (2018).
[5] F. Stollmeier and J. Nagler, *Physical review letters* **120**, 058101 (2018).
[6] X.-D. Zheng, C. Li, S. Lessard, and Y. Tao, *Physical*

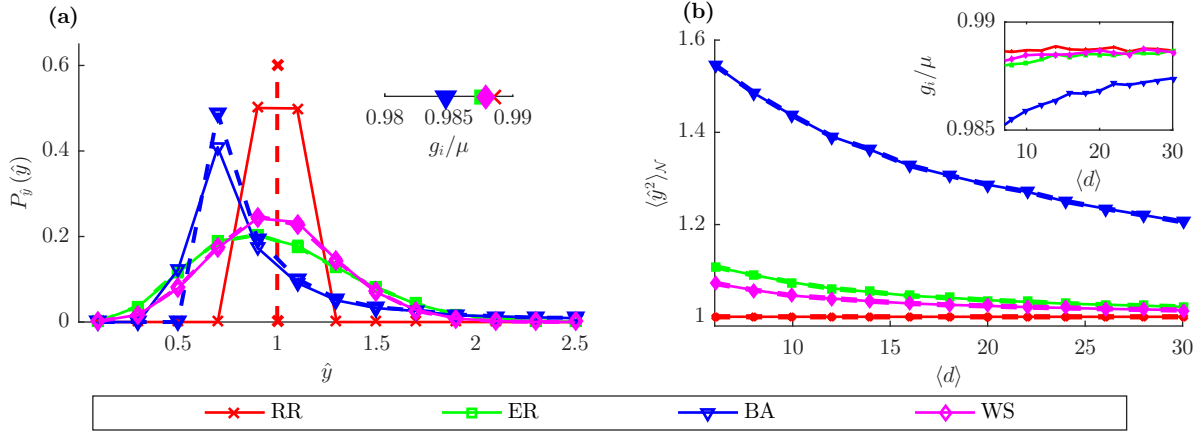


FIG. 4. **Numerical analysis.** (a) Estimated PDF for the rescaled resources for four different types of random graphs – RR, ER, WS and BA, each having an average degree $\langle d \rangle = 5$. The inset plot depicts the ratio of the estimated growth rate and the drift parameter for the same graphs. (b) The variance of rescaled wealth as a function of the average degree $\langle d \rangle$ for the same graphs. The corresponding g_i/μ ratios are depicted in the inset. (a-b) Filled lines represent the simulated values while the dashed lines are the analytical solutions of the corresponding variables. In the simulation $\mu = 0.3$ and $\sigma^2 = 0.4$. For each graph type, the results are averaged across 100 realizations. The graphs contain 100 individuals involved in pooling and sharing.

review letters **120**, 218101 (2018).

[7] I. Cvijović, B. H. Good, E. R. Jerison, and M. M. Desai, Proceedings of the National Academy of Sciences **112**, E5021 (2015).

[8] J. Aitchison and J. A. Brown, (1957).

[9] S. Redner, American Journal of Physics **58**, 267 (1990).

[10] O. Peters and M. Gell-Mann, Chaos: An Interdisciplinary Journal of Nonlinear Science **26**, 023103 (2016).

[11] B.-E. Sæther and S. Engen, Trends in ecology & evolution **30**, 273 (2015).

[12] G. Yaari and S. Solomon, The European Physical Journal B **73**, 625 (2010).

[13] T. Liebmann, S. Kassberger, and M. Hellmich, European Journal of Operational Research **258**, 193 (2017).

[14] O. Peters and A. Adamou, arXiv preprint arXiv:1506.03414 (2015).

[15] M. B. Short, C. A. Solari, S. Ganguly, T. R. Powers, J. O. Kessler, and R. E. Goldstein, Proceedings of the National Academy of Sciences **103**, 8315 (2006).

[16] M. Roper, M. J. Dayel, R. E. Pepper, and M. Koehl, Physical review letters **110**, 228104 (2013).

[17] K. L. Adam, *Community supported agriculture* (ATTRA-National Sustainable Agriculture Information Service Butte, MT, 2006).

[18] A. Sapir, P. Aghion, G. Bertola, M. Hellwig, J. Pisani-Ferry, D. Rosati, J. Viñals, H. Wallace, M. Buti, M. Nava, *et al.*, *An agenda for a growing Europe: The Sapir report* (OUP Oxford, 2004).

[19] J. E. Stiglitz, R. M. Sapsolsky, V. Eubanks, J. K. Boyce, B. Rothstein, J. Redden, and M. Szalavitz, Scientific American **Special Report** (2018).

[20] B. Allen, G. Lippner, Y.-T. Chen, B. Fotouhi, N. Momeni, S.-T. Yau, and M. A. Nowak, Nature **544**, 227 (2017).

[21] M. Perc, J. Gómez-Gardeñes, A. Szolnoki, L. M. Floría, and Y. Moreno, Journal of the royal society interface **10**, 20120997 (2013).

[22] F. C. Santos, M. D. Santos, and J. M. Pacheco, Nature **454**, 213 (2008).

[23] V. Stojkoski, Z. Utkovski, L. Basnarkov, and L. Kocarev, Physical Review E **97**, 052305 (2018).

[24] J.-P. Bouchaud and M. Mézard, Physica A: Statistical Mechanics and its Applications **282**, 536 (2000).

[25] D. Garlaschelli and M. I. Loffredo, Journal of Physics A: Mathematical and Theoretical **41**, 224018 (2008).

[26] Y. Berman, O. Peters, and A. Adamou, (2017).

[27] T. Ichinomiya, Physical Review E **86**, 066115 (2012).

[28] O. Peters and A. Adamou, arXiv preprint arXiv:1802.02939 (2018).

[29] The distribution of resources in non-cooperating GBM trajectories is log-normal.

[30] B. Bollobás, *Modern graph theory*, Vol. 184 (Springer Science & Business Media, 2013).

[31] P. Erdos and A. Rényi, Publ. Math. Inst. Hung. Acad. Sci **5**, 17 (1960).

[32] D. J. Watts and S. H. Strogatz, nature **393**, 440 (1998).

[33] A.-L. Barabási and R. Albert, science **286**, 509 (1999).

[34] A. D. Broido and A. Clauset, arXiv preprint arXiv:1801.03400 (2018).

[35] A. Clauset, C. R. Shalizi, and M. E. Newman, SIAM review **51**, 661 (2009).

[36] M. J. Salganik, P. S. Dodds, and D. J. Watts, science **311**, 854 (2006).

[37] A. Nishi, H. Shirado, D. G. Rand, and N. A. Christakis, Nature **526**, 426 (2015).

[38] Y.-S. Chiang, PloS one **10**, e0128777 (2015).

[39] M. Tsvetkova, C. Wagner, and A. Mao, PloS one **13**, e0200965 (2018).

[40] O. Peters, Quantitative Finance **11**, 1593 (2011).

[41] D. Herzer and S. Vollmer, The Journal of Economic Inequality **10**, 489 (2012).

[42] Z. Utkovski, V. Stojkoski, L. Basnarkov, and L. Kocarev, Physical Review E **96**, 022315 (2017).

[43] V. Stojkoski, Z. Utkovski, E. Andre, and L. Kocarev, arXiv preprint arXiv:1805.09101 (2018).